

COORDINATED CONTROL OF TETHERED SATELLITE CLUSTER SYSTEMS

Osamu MORI* and Saburo MATUNAGA**

Tokyo Institute of Technology, 2-12-1 Ookayama, Meguro-ku, Tokyo, 152-8552, JAPAN

Abstract

We propose the concept of Tethered Satellite Cluster Systems, which keep and change the constellation with the tension/length control of tethers. The purpose of the system is the formation flight to perform the observation, communication and rendezvous-docking missions. The system is applied to tethered service satellites, which perform the missions, for example an automatic casting, capture, recovery, moorage and deorbit of an uncontrolled satellite.

In this paper, we consider the rotating motion of this system for the interferometry mission. This system can save the fuel of the thruster in the rotating motion around the center of the mass of the system in orbit, because the tether tension supplies the control force. By numerical simulations, we establish the coordinated control method and analyze the case where three satellites are joined by three tethers. By two-dimensional ground experiments, we indicate that the tether tension save the fuel of the thruster for driving the rotating motion.

* Research Associate, Dept. of Mechanical and Aerospace Eng., Member AIAA

** Associate Professor, Dept. of Mechanical and Aerospace Eng., Member AIAA

Introduction

We propose the concept of Tethered Satellite Cluster Systems^[1], which keep and change the constellation with the tension/length control of tethers. The purpose of the system is the formation flight to perform the observation, communication and rendezvous-docking missions as shown in figure 1. The system is applied to tethered service satellites, which perform the missions, for example an automatic casting, capture, recovery, moorage and deorbit of an uncontrolled satellite as shown in figure 2^{[2][3]}.

NASA considers the satellite formation flying for the interferometry mission in Space Technology 3, and Randal W. Beard and Fred Y. Hadaegh derived control laws for rotating a constellation of spacecraft using on/off thrusters^[4]. Existing system, however, needs a lot of fuel of the thruster for rotating motion. On the other hand, tether satellite cluster systems can save the fuel, because the tether tension supplies the control force. In this paper, we analyze the rotating motion around the center of the mass of the system in orbit and establish the coordinated control method by numerical simulations. In addition, we outline a ground experiment system including the reel mechanism for the tethered satellite cluster systems, and verify the advantage of saving the fuel of the thruster with use of tether tension by two-dimensional experiments. Finally, we indicate the future works.

Tethered Satellite Cluster Systems

Figure 3 shows the concept of tethered satellite cluster systems. The features of the system are as follows.

- (1) The system keeps and changes the constellation by satellites joint/separation with tether.
- (2) The tether tension/length is controlled by a reel mechanism, and the satellites

joint/separation is conducted by joint mechanism.

(3) The reel or joint mechanism is installed in the arms on each satellite.

(4) Each satellite conducts coordinated control of position and attitude.

As most fundamental motion of the system, we consider following two motions.

(a) Translating motion: to move the object to arbitrary position.

This motion is applied to the rendezvous-docking mission. We already analyzed the dynamics of two satellites joined by a tether in inertial coordinate system and established the tension control method for equalizing two satellites in the velocity magnitude without exciting the attitude vibration of each satellite^[5].

(b) Rotating motion: to spin the system for keeping or changing the constellation.

This motion is applied to the interferometry mission. Existing system needs a lot of fuel of the thruster for rotating motion. This system, however, save the fuel, because the tether tension supplies the control force. In this paper, we analyze the rotating motion of this system in orbit and verify the advantage.

Combining two motions, the system performs various applied missions, for example attitude control of an uncontrolled satellite.

Modeling and Formulation

The dynamical model and formulation of the tethered satellite cluster systems is as follows. Figure 4 shows an analytical model. The motion of the n satellites joined by tethers in earth-centered inertial coordinate system $\{\mathbf{i}\}$ is considered. The following assumptions are made.

Satellite j ($j=1, \dots, n$):

The mass is m_j ; the position of the center of the mass is \mathbf{q}_j ; the moment of inertia is \mathbf{I}_j ; the angular velocity with respect to $\{\mathbf{i}\}$ is $\boldsymbol{\omega}_j$; and the body-fixed coordinate system is $\{\mathbf{b}_j\}$.

Tether jk (Tether kj):

The tether joins satellite j and satellite k . The tension is T_{jk} ($=T_{kj}$); the mass, twist and bending moment, and tensile strain are ignored.

Arm jk :

The arm joins tether jk on the satellite j . The arm controls the joint (reel or joint mechanism) position \mathbf{a}_{jk} ($\neq \mathbf{a}_{kj}$) arbitrarily.

By Newton-Euler equations, the motion of each satellite in circular orbit is formulated as follows.

$$m_j \ddot{\mathbf{q}}_j = \frac{\mu m_j}{|\mathbf{q}_j|^3} \mathbf{q}_j + \sum_k \mathbf{T}_{jk} \quad (1)$$

$$\mathbf{I}_j \cdot \dot{\boldsymbol{\omega}}_j + \boldsymbol{\omega}_j \times \mathbf{I}_j \cdot \boldsymbol{\omega}_j = \frac{3\Omega^2}{|\mathbf{q}_j|^2} \mathbf{q}_j \times \mathbf{I}_j \cdot \mathbf{q}_j + \sum_k \boldsymbol{\tau}_{jk} \quad (2)$$

where Ω is the orbital angular velocity; \mathbf{T}_{jk} and $\boldsymbol{\tau}_{jk}$ are tension and torque vector working on satellite j by tether jk .

$$\mathbf{T}_{jk} = T_{jk} \frac{(\mathbf{q}_k + \mathbf{r}_{kj}) - (\mathbf{q}_j + \mathbf{r}_{jk})}{|(\mathbf{q}_k + \mathbf{r}_{kj}) - (\mathbf{q}_j + \mathbf{r}_{jk})|} \quad (3)$$

$$\boldsymbol{\tau}_{jk} = \mathbf{a}_{jk} \times \mathbf{T}_{jk} \quad (4)$$

Rotating Motion

We assume that all satellites in the system are joined by tethers, and establish the coordinated control for the rotating motion where all satellites rotate around the center of the mass of the system in same plane at same angular velocity.

Rotating Coordinate System

Figure 5 shows the simulation model ($n = 3$). We define the rotating coordinate system $\{\mathbf{r}\}$ as follows.

The origin is the center of the mass of the system.

$$\mathbf{q}_{\text{c.m.}} = \frac{\sum_{j=1}^n m_j \mathbf{q}_j}{\sum_{j=1}^n m_j} \quad (5)$$

\mathbf{r}_z axis shows the direction of the angular momentum of the system on the origin.

$$\mathbf{P} \equiv \sum_{j=1}^n \{m_j (\mathbf{q}_j - \mathbf{q}_{\text{c.m.}}) \times (\dot{\mathbf{q}}_j - \dot{\mathbf{q}}_{\text{c.m.}}) + \mathbf{I}_j \cdot \boldsymbol{\omega}_j\} \quad (6)$$

\mathbf{r}_x axis shows the direction of satellite 1 in $\mathbf{r}_x \mathbf{r}_y$ plane.

The relationship between $\{\mathbf{r}\}$ and $\{\mathbf{i}\}$ is defined by Euler angles.

$$\{\mathbf{r}\} = C^3(\varphi_r) C^2(\theta_r) C^1(\psi_r) \{\mathbf{i}\} \quad (7)$$

We call $\mathbf{r}_x \mathbf{r}_y$ plane rotating plane.

Position/Attitude

The position and attitude of each satellite in $\{\mathbf{r}\}$ is defined as follows.

$$\text{Position: } \mathbf{q}_j - \mathbf{q}_{\text{c.m.}} = \{\mathbf{r}\}^T \begin{bmatrix} d_j \cos \lambda_j \\ d_j \sin \lambda_j \\ h_j \end{bmatrix} \quad (8)$$

$$\text{Attitude: } \{\mathbf{b}_j\} = C^1(\psi_j)C^2(\theta_j)C^3(\varphi_j)\{\mathbf{r}\} \quad (9)$$

Where, d_j is the distance between satellite j and \mathbf{r}_z axis; λ_j is the angle between satellite j and \mathbf{r}_x axis in rotating plane; and h_j is the height of satellite j out of rotating plane. Because of definition of $\{\mathbf{r}\}$, these values satisfy the following equations.

$$\sum_{j=1}^n m_j \begin{bmatrix} d_j \cos \lambda_j \\ d_j \sin \lambda_j \\ h_j \end{bmatrix} = \begin{bmatrix} 0 \\ 0 \\ 0 \end{bmatrix} \quad (10)$$

$$\lambda_1 = 0 \quad (11)$$

The objective position/attitude is denoted by a superscript d : d_j^d , for example. In objective rotating motion, the distance L_{jk} between satellite j and satellite k , and the angular velocity ω_r are represented as follows.

$$L_{jk} = d_j^{d^2} + d_k^{d^2} - 2d_j^d d_k^d \cos(\lambda_k^d - \lambda_j^d) \quad (12)$$

$$\omega_r \mathbf{r}_z = \frac{\mathbf{P}}{\sum_{j=1}^n (m_j d_j^{d^2} + |\mathbf{I}_j^d \cdot \mathbf{r}_z|)} \quad (13)$$

Because of the condition of the rotating motion, the following equation is satisfied.

$$h_j^d = 0 \quad (14)$$

Coordinated Control Method

We establish the control method for rotating motion. First, we consider the conditions

that each satellite is stable in objective position/attitude dynamically.

Condition 1: The sum of the tether tensions working on each satellite is equal to the centrifugal force for rotating motion in objective position. The centrifugal tension is represented as follows.

$$T_{jk}^d = \frac{m_j m_k L_{jk} \omega_r^2}{\sum_{l=1}^n m_l} \quad (15)$$

Note that the condition 1 is satisfied in case of all satellites in the system are joined by tethers.

Condition 2: The arm direction is equal to the tether direction in objective position/attitude in order that the tether torque working on the satellite is equal to zero. The joint vector satisfies following equation.

$$\mathbf{a}_{jk}^d \times T_{jk} (\mathbf{q}_k^d - \mathbf{q}_j^d) = 0 \quad (16)$$

Figure 7 shows the equilibrium of satellite 1 in case of $n = 3$.

By the items mentioned above, we propose the coordinated control method for transition to objective position/attitude.

$$\text{Tension control: } T_{jk} = T_{jk}^d [1 + k_1 \Delta L + k_2 \Delta \dot{L} - k_3 \Delta \omega] \quad (17)$$

$$\text{Arm control: } \mathbf{a}_{jk}^d = l_{jk} \frac{\mathbf{q}_k^d - \mathbf{q}_j^d}{|\mathbf{q}_k^d - \mathbf{q}_j^d|} \quad (18)$$

Where, k_1 and k_2 are the coefficients for correcting position, and k_3 is that for correcting attitude. The errors of distance, velocity and angular velocity between satellite j and satellite k are as follows.

$$\Delta L = \left(\left| \mathbf{q}_k - \mathbf{q}_j \right| - L_{jk} \right) \quad (19)$$

$$\Delta \dot{L} = \left(\dot{\mathbf{q}}_k - \dot{\mathbf{q}}_j \right) \cdot \left(\mathbf{q}_k - \mathbf{q}_j \right) / \left| \mathbf{q}_k - \mathbf{q}_j \right| \quad (20)$$

$$\Delta \boldsymbol{\omega} = \left\{ \boldsymbol{\tau}_{jk} \times \left(\boldsymbol{\omega}_j - \boldsymbol{\omega}_r \mathbf{r}_z \right) + \boldsymbol{\tau}_{kj} \times \left(\boldsymbol{\omega}_k - \boldsymbol{\omega}_r \mathbf{r}_z \right) \right\} \cdot \mathbf{r}_z \quad (21)$$

l_{jk} shows the distance between tether joint and center of the satellite j . Note that the tether torque working on each satellite is proportional to l_{jk} .

Numerical Simulations

We analyze the rotating motion in case of $n=3$ and verify the coordinated control method by numerical simulations.

Simulation Conditions

The simulation conditions are as follows.

Condition 1: The orbital angular velocity of the center of the system (height: 350 km, period: 5492 s) is

$$\Omega = 0.001144 \text{ rad/s} . \quad (22)$$

Condition 2: The shape of each satellite is

$$m_j = 50 \text{ kg} , \quad I_j = \begin{bmatrix} 10 & 0 & 0 \\ 0 & 10 & 0 \\ 0 & 0 & 10 \end{bmatrix} \text{ kgm}^2 . \quad (23)$$

Condition 3: The objective position and attitude of each satellite are

$$d_1^d = 20 \text{ m} , \quad d_2^d = d_3^d = 10\sqrt{2} \text{ m} \quad (24)$$

$$\lambda_2^d = 3\pi / 4 \text{ rad} , \quad \lambda_3^d = 5\pi / 4 \text{ rad} \quad (25)$$

$$\varphi_j^d = \theta_j^d = \psi_j^d = 0 \text{ rad} . \quad (26)$$

The objective formation is the isosceles triangle.

Condition 4: The initial attitude of the rotating plane is

$$\psi_{r0} = \pi / 6 \text{ rad} , \quad \theta_{r0} = \pi / 6 \text{ rad} , \quad \varphi_{r0} = 0 \text{ rad} . \quad (27)$$

The initial position/attitude of each satellite is defined by $d_{j0}, \lambda_{j0}, h_{j0} / \varphi_{j0}, \theta_{j0}, \psi_{j0}$. The initial angular velocities of all satellites are same: $\omega_0 \mathbf{r}_z$. Thus we consider the following $(6n+4)$ parameters in numerical simulations. When we do not show these values, we set them as follows.

$$\{\omega_0, d_{j0}, \lambda_{j0}, h_{j0}, \varphi_{j0}, \theta_{j0}, \psi_{j0}, k_1, k_2, k_3\}^T = \{20\Omega, d_j^d, \lambda_j^d, h_j^d, \varphi_j^d, \theta_j^d, \psi_j^d, 0.5, 0.5, 1000\}^T \quad (28)$$

In numerical simulations, we assume that each arm is controlled and equations (18) and (29) are satisfied in order to verify tension control method.

$$l_{jk} = 1 \text{ m} \quad (29)$$

Rotating Plane Motion

First, we analyze the rotating plane motion with respect to various ω_0 . Figure 8 shows the transition of ψ_r, θ_r and $\dot{\varphi}_r$ in an orbital period. Each line shows data when ω_0 is set as follows.

$$\text{Solid line: } \omega_0 = 20\Omega \quad (30)$$

$$\text{Broken line: } \omega_0 = 10\Omega \quad (31)$$

$$\text{Dotted line: } \omega_0 = 5\Omega \quad (32)$$

The solid line satisfies the following equations.

$$\psi_r \approx \psi_{r0}, \quad \theta_r \approx \theta_{r0}, \quad \dot{\phi}_r \approx \omega_0 \quad (33)$$

These lines show that, when $\omega_r \gg \Omega$ is satisfied, the influence of gravitation can be ignored and rotating plane motion becomes constant. In following section, we set $\omega_0 = 20\Omega$ in order to simplify the rotating motion. Note that Steven Steven G. Tragesser considered the stability based on the conical Likins-Pringle relative equilibrium for keeping the spin axis of the formation roughly pointed toward the Earth^[6].

Position Control

Next, we consider the position control when the initial formation is the following triangle leaning from rotating plane.

$$d_{10} = d_{20} = d_{30} = 10 \text{ m} \quad (34)$$

$$\lambda_{10} = 0 \text{ rad}, \quad \lambda_{20} = 2\pi/3 \text{ rad}, \quad \lambda_{30} = 4\pi/3 \text{ rad} \quad (35)$$

$$h_{10} = -1 \text{ m}, \quad h_{20} = 0.5 \text{ m}, \quad h_{30} = 0.5 \text{ m} \quad (36)$$

Figure 9 shows the graphs of d_2, λ_2 and h_2 in an orbital period. Each line shows the following case.

$$\text{Solid line: } k_1 = 0.5, \quad k_2 = 0.5 \quad (37)$$

$$\text{Broken line: } k_1 = 0, \quad k_2 = 0 \quad (38)$$

Figure 10 shows the constellation transition in former case. The solid line shows that satellite 2 can change the objective position in rotating plane. This is the effect of the tension for correcting position. The vibration out of rotating plane, however, cannot be damped, because tether direction is perpendicular to vibration direction. The transitional inclination of satellites 1 and 3 is nearly equal to that of satellite 2.

Attitude Control

Finally, we investigate the attitude control when the initial attitude of satellite 2 is not equal to the objective attitude as follows.

$$\varphi_2 = \pi/9, \quad \theta_2 = \pi/9, \quad \psi_2 = \pi/9 \quad (39)$$

Figure 11 shows the data of φ_2, θ_2 and ψ_2 . We analyze two cases as follows.

$$\text{Solid line: } k_3 = 1000 \quad (40)$$

$$\text{Broken line: } k_3 = 0 \quad (41)$$

Figure 12 shows the attitude transition of satellite 2 in former case. The attitude vibration on center of objective attitude can be decreased by the tension for correcting attitude. We assume that tether torque working on the satellite is equal to zero in this simulation. Therefore, the attitude of satellite can change objective attitude by the coordinate control of arm and tension.

Thruster Control

This system has the advantages of supplying the driving force to each satellite by tension. The thrust for keeping object position/attitude of each satellite in rotating motion is

$$F_j = m_j d_j^d \omega_r^2. \quad (42)$$

In numerical simulation, the thrust for rotating motion of satellite 2 is 0.370 N. When the specific impulse is 220 s, the fuel of thruster per an orbital period is 0.943 kg. It is about as much as 2 percent of mass of satellite 2, and it can be saved by the system with tether tension. Tether tension is, however, the internal force of the whole system, thus the thruster is required for the following control.

1. Control of the orbital motion of the system.

2. Control of the rotating plane motion.
3. Control of the motion of out of rotating plane.

In numerical simulations, we analyze the case of $n=3$. In the other case, following problem is occurred.

In case of $n=2$: Each satellite is joined by only one tether as shown in figure 13. The rotating motion on the tether cannot be controlled, because the twist moment of the tether is ignored. Thus, the torque is necessary for control of the rotating motion.

In case of $n \geq 4$: The interaction between tethers cannot be ignored, because tethers are crossed as shown in figure 14.

Ground Experiments

We verify the advantage of saving the fuel of the thruster for rotating motion in case of $n=2$ by two-dimensional ground experiments.

Ground Experiment System

Figure 15 shows the concept of two-dimensional ground experiment system. This system consists of three subsystems: satellites 1, 2 and ground station.

Figure 16 shows the picture of each subsystem. The outline is as follows.

Satellites 1 and 2: Each satellite is the rectangular solid (0.6 m \times 0.6 m \times 0.45 m), floating on the flat floor (3 m \times 5 m) with air pad. It obtains the driving force with tether tension and thruster. The air for floating pad thrust is supplied by tank (20 atm). The gyro acquires the attitude data of the satellite and the PC communicates with the ground station by wireless LAN (TCP/IP protocol). In addition, the reel mechanism, installed on satellite 1 controls

tether tension. The mass of each satellite is

$$m_1 = 58 \text{ kg} , m_2 = 42 \text{ kg} . \quad (43)$$

Ground Station: The CCD camera gains the pictures of the whole flat floor and the PC calculates the position of satellites 1 and 2 by pattern matching. The Joy Stick controls the position/attitude of each satellite through the wireless network.

Reel Mechanism

Tether control system consists of reel and joint mechanisms. In this paper, the reel mechanism is considered.

The most fundamental function of the reel mechanism is to deploy and retract the tether. But the reel mechanism for the tethered satellite cluster systems needs the following functions as well.

- (1) To avoid jam in the case where tension is nearly zero.
- (2) To measure tension and direction of the tether.
- (3) To wind the tether on the reel uniformly.
- (4) To measure deployed length of the tether.

Taking into account those requirements, we developed the reel mechanism for ground experiment as shown in Figure 17. The size is 140 mm × 400 mm × 200 mm and the weight is 3.95 kg. Each function is realized as follows.

- (1) The reel mechanism is separated into two parts: an inner mechanism and an outer mechanism. In the inner mechanism, motor A deploys and retracts the tether under the specified constant tension. In the outer mechanism, motor B conducts tension/length control of the tether.

(2) Strain gage A measures the inner tension, strain gage B measures the outer tension, and strain gage C measures the direction of deployed tether.

(3) By a level winder, a winded point moves periodically and winds the tether on the reel uniformly.

(4) A laser displacement sensor measures tether-winding thickness and an encoder measures the reel rotation.

Results of Ground Experiment

We conduct the ground experiment in which two satellites face each other and rotate around the center of the system as follows.

$$\text{Angular velocity: } \omega_r = 0.0698 \text{ rad/s (Period: 90 s)} \quad (44)$$

$$\text{Rotating radius: } d_1^d = 0.88 \text{ m, } d_2^d = 1.22 \text{ m} \quad (45)$$

The initial velocity and angular velocity of each satellite satisfy the condition of the rotating motion. Figure 18 shows the attitude angle and fuel consumption of satellite 1 in one round, respectively. We conduct two experiments as follows.

$$\text{Solid line (this system): } T = m_j d_j^d \omega_r^2 = 0.25 \text{ N} \quad (46)$$

$$\text{Broken line (existing system): } T = 0 \text{ N} \quad (47)$$

In figure 18 (a), two lines are nearly equal and increase linearly to 2 in about 90 s. Thus, both cases satisfy the objective rotating motion. On the other hand, in figure 18 (b), the value of the solid line is smaller than that of the broken line. The former is not equal to zero, for the friction between each satellite and flat floor damps the rotating motion. The difference between the latter and the former is nearly equal to the gas consumption of thruster for driving the central force. Therefore, we conclude that the tension can save the

fuel of thruster.

Conclusions

In this paper, we consider the rotating motion of tethered satellite cluster systems as follows.

1. By numerical simulations, we established the coordinated control method and analyzed the case where three satellites were joined by tether.
2. By two-dimensional ground experiments, we indicated that the tether tension saved the fuel of the thruster for driving the rotating motion in this system.

Future Works

Finally, we show the future works.

(1) Formation flight experiment:

As shown in figure 19, we will conduct the rotating experiment of three satellites joined by three tethers in order to verify the advantage of saving the fuel of the thruster.

(2) Reconfigurable analysis

We will analyze the motion of the system transition from close-loop configuration to open-loop configuration by tether separation.

(3) Tether service experiment:

We are developing the arm system for ground experiment. We will conduct the application experiments for attitude control of uncontrolled satellite with use of tension and arm control as shown in figure 20.

REFERENCES

- [1] S. Matunaga, O. Mori, T. Kanzawa, S. Tsurumi and N. Maeda, "Concept of Robot Satellite Cluster and Ground Experiment System," *Proceedings of TITech COE/Super Mechano-Systems Workshop 2000*, Feb. 2-3, Tokyo, 2000, pp.103-111.
- [2] S. Matunaga, O. Mori and Y. Ohkami, "Dynamics of Tethered Multibody Systems with Friction and Impact," *AIAA Guidance, Navigation, and Control Conference and Exhibit*, Part 1, Boston, Aug. 10-12, 1998, pp.278-285.
- [3] O. Mori and S. Matunaga, "Dynamics of Capturing Uncontrolled Satellite with Tether," *43rd Space Sciences and Technology Conference*, Oct. 20-22, Kobe, 1999, 99-1A5, pp.37-42. (in Japanese)
- [4] Randal W. Beard and Fred Y. Hadaegh, "Finite Thrust Control for Satellite Formation Flying with State Constraints," ACC99-IEEE0173.
- [5] O. Mori and S. Matunaga, "Tension Control Tethered Satellite Cluster," *22nd International Symposium on Space Technology and Science*, Morioka, May 28-June 4, 2000, 2000-k-21, pp.1786-1794.
- [6] Steven G. Tragesser, "Formation Flying with Tethered Spacecraft," *AIAA/AAS Astrodynamics Specialist Conference*, Aug. 14-17, Denver, 2000, AIAA2000-4133.

List of Figures

- Fig. 1 Formation Flight
- Fig. 2 Tether Service Satellite
- Fig. 3 Tether Satellite Cluster Systems
- Fig. 4 Analytical Model
- Fig. 5 Rotating Coordinate System
- Fig. 6 Constellation
- Fig. 7 Equilibrium of Satellite 1
- Fig. 8 Rotating Plane Motion
- Fig. 9 Position Control
- Fig. 10 Constellation Transition
- Fig. 11 Attitude Control
- Fig. 12 Attitude Transition of Satellite 2
- Fig. 13 Tether Twist ($n = 2$)
- Fig. 14 Interaction between Tethers ($n = 4$)
- Fig. 15 Ground Experiment System
- Fig. 16 Subsystems
- Fig. 17 Reel Mechanism
- Fig. 18 Experiment Results of Satellite 1
- Fig. 19 Formation Flight Experiment
- Fig. 20 Tether Service Experiment

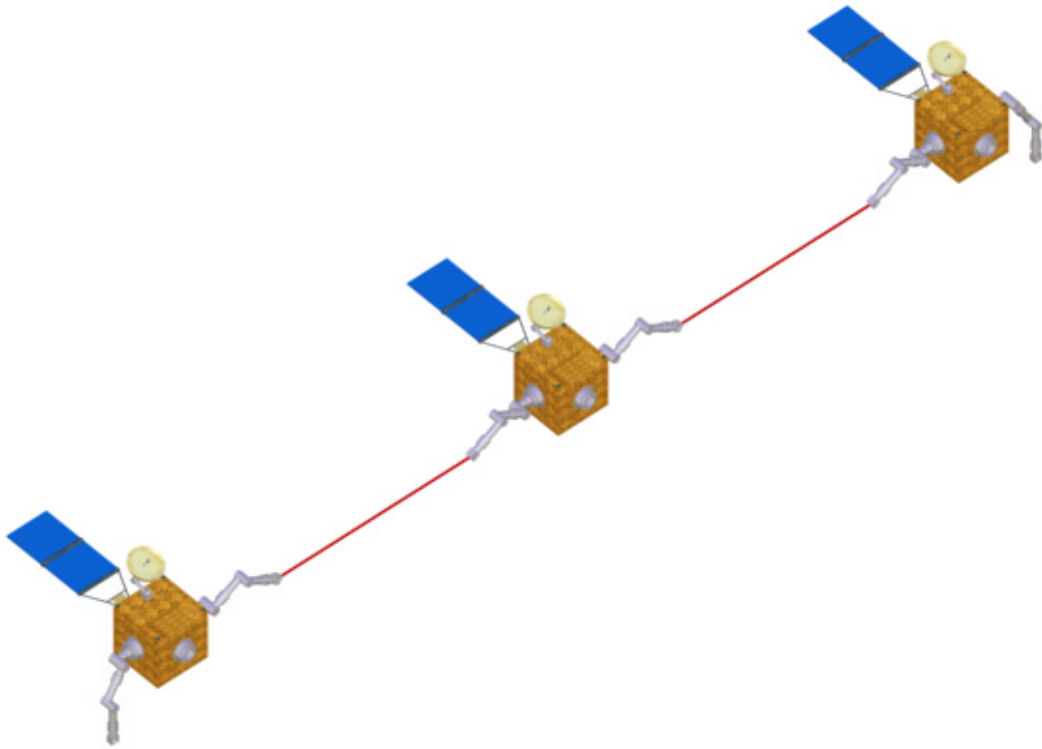


Fig. 1 Formation Flight

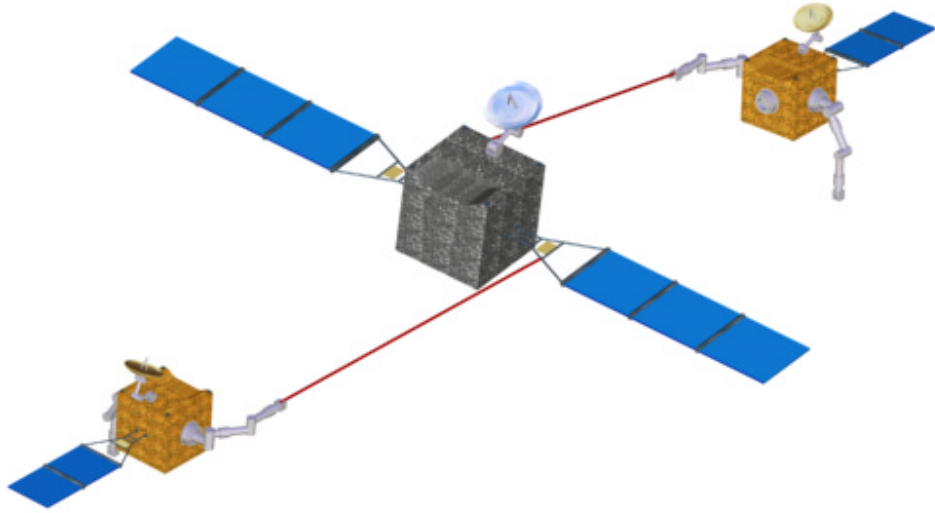


Fig. 2 Tether Service Satellite

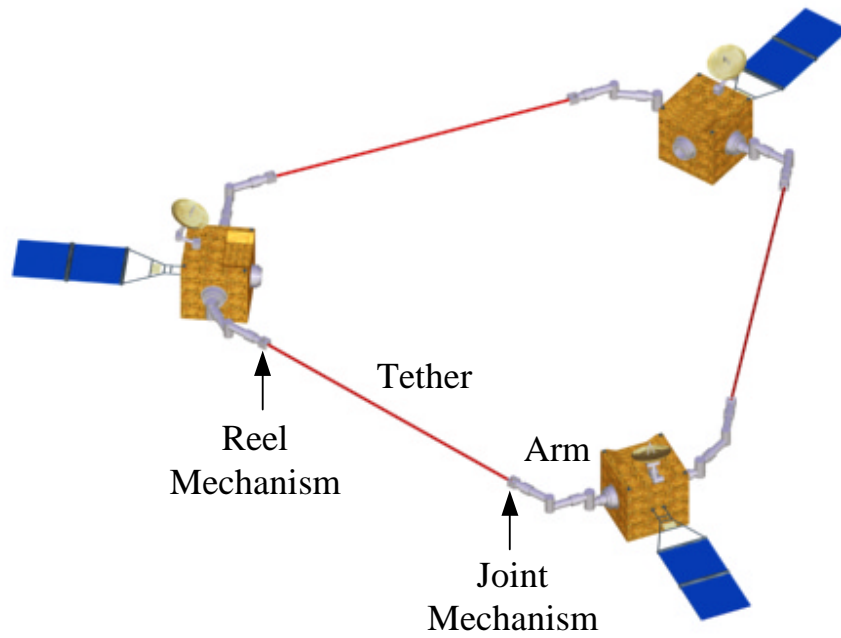


Fig. 3 Tether Satellite Cluster Systems

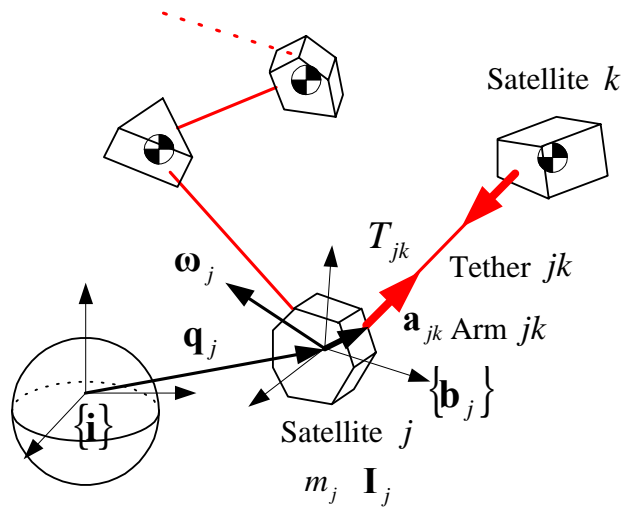


Fig. 4 Analytical Model

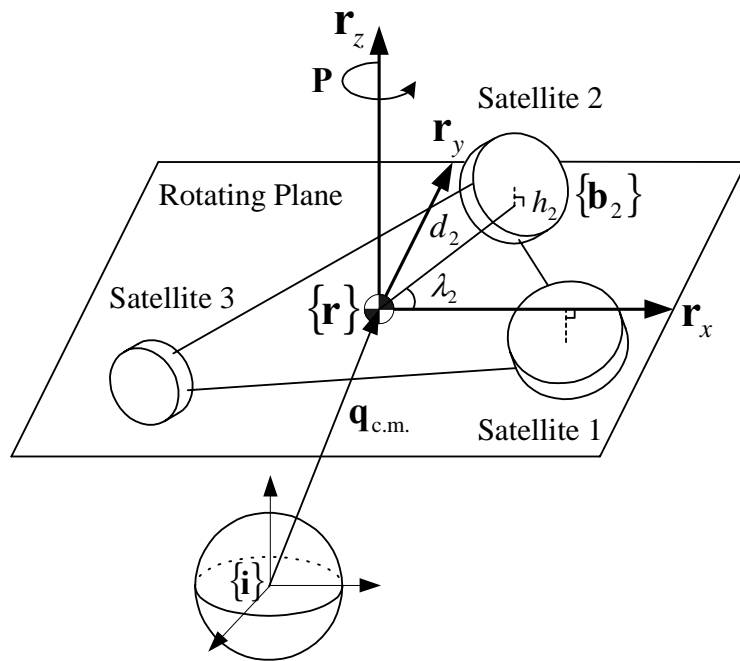


Fig. 5 Rotating Coordinate System

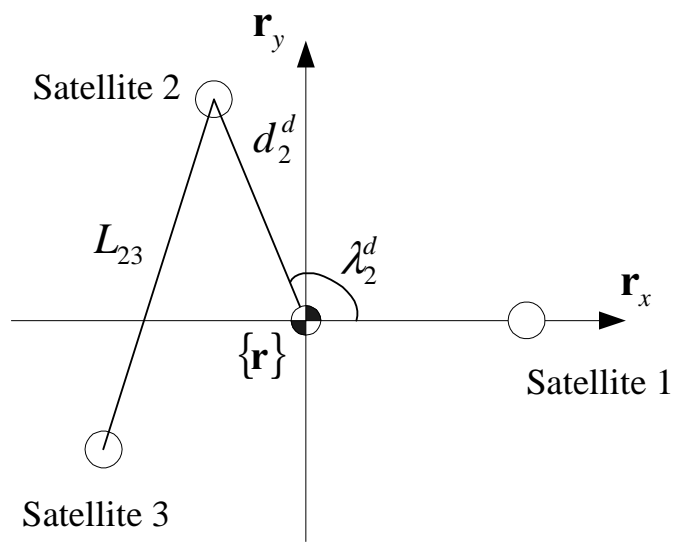


Fig. 6 Constellation

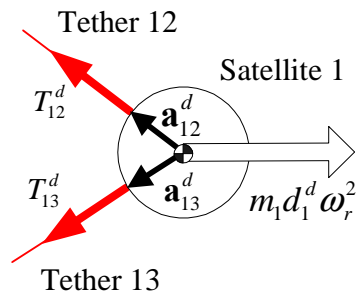
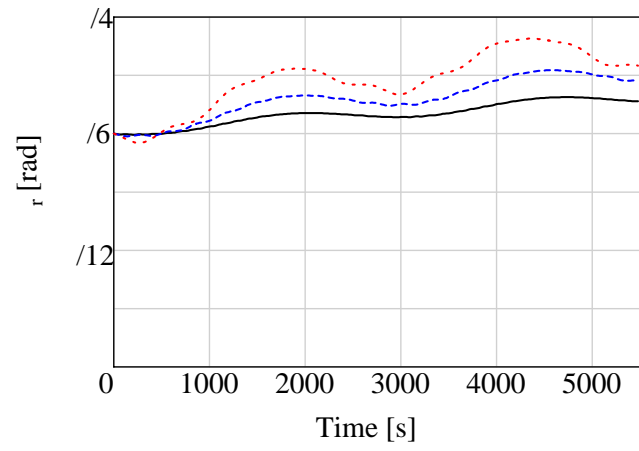
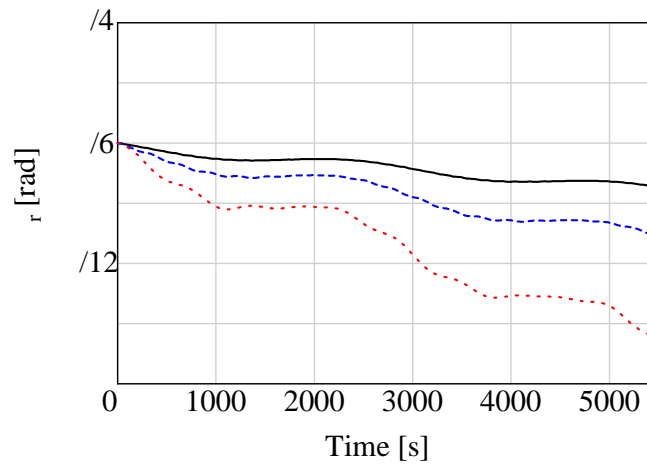


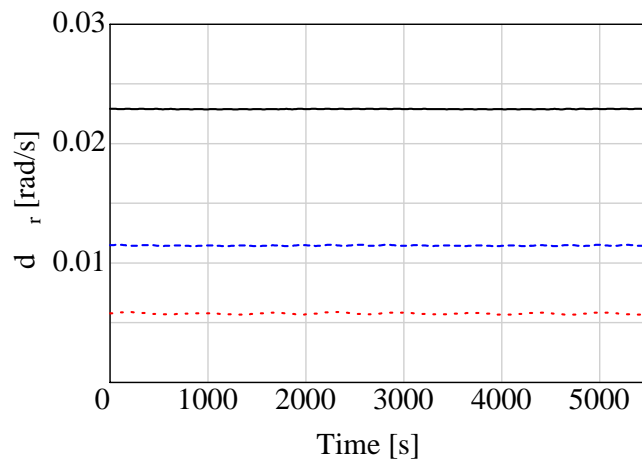
Fig.7 Equilibrium of Satellite 1



(a) ψ_r

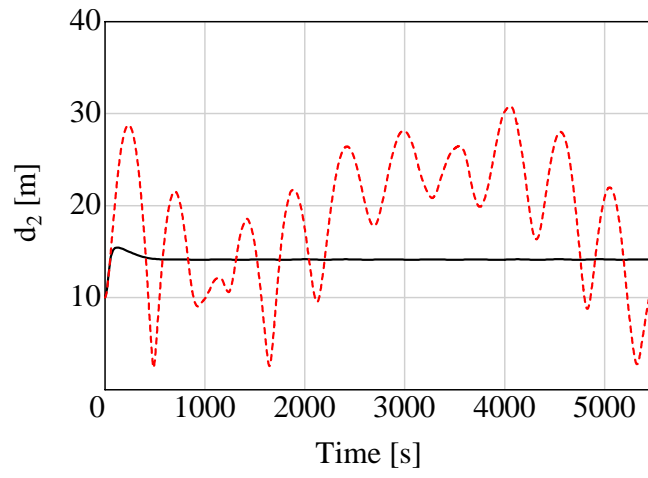


(b) θ_r

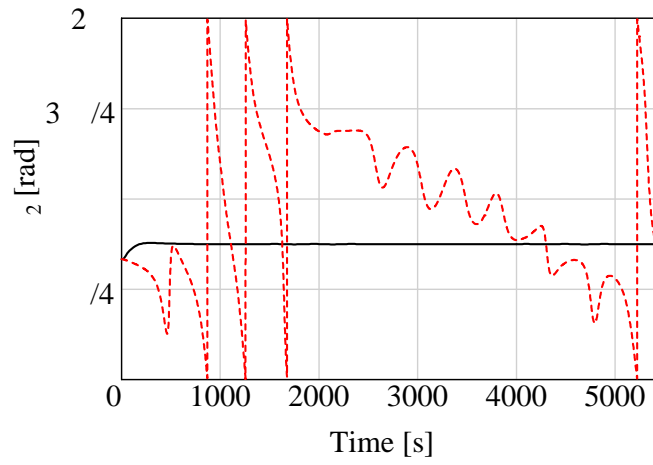


(c) $\dot{\phi}_r$

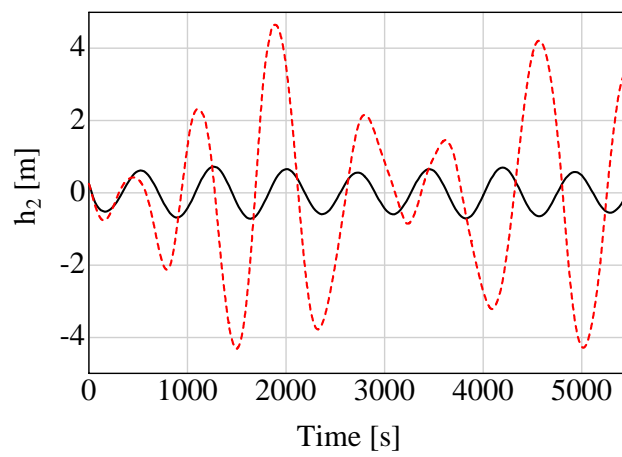
Fig. 8 Rotating Plane Motion



(a) d_2



(b) λ_2



(c) h_2

Fig. 9 Position Control

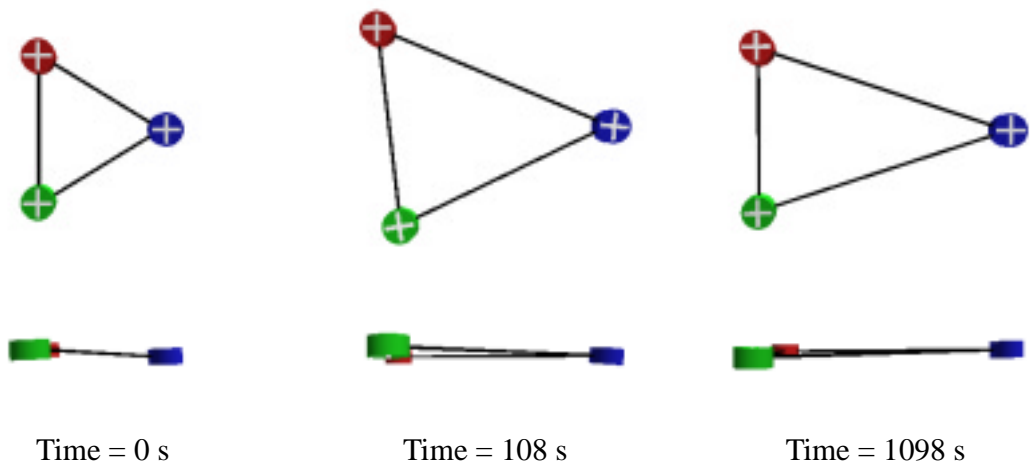
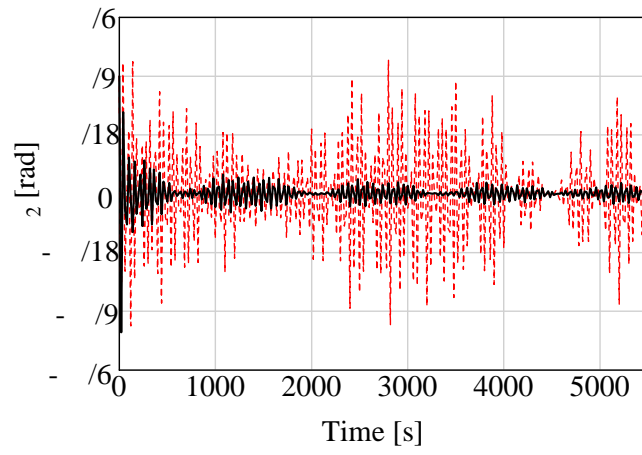
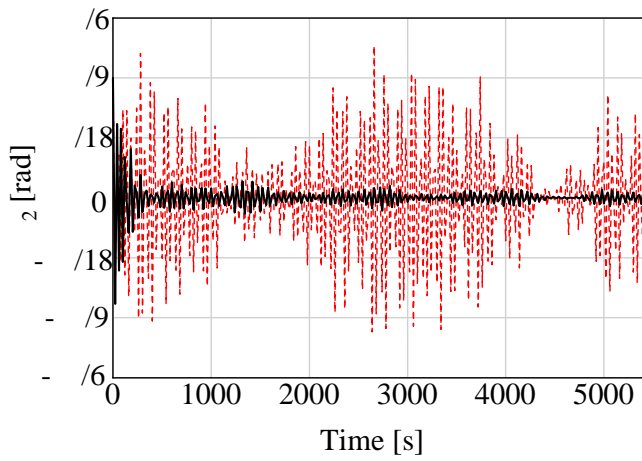


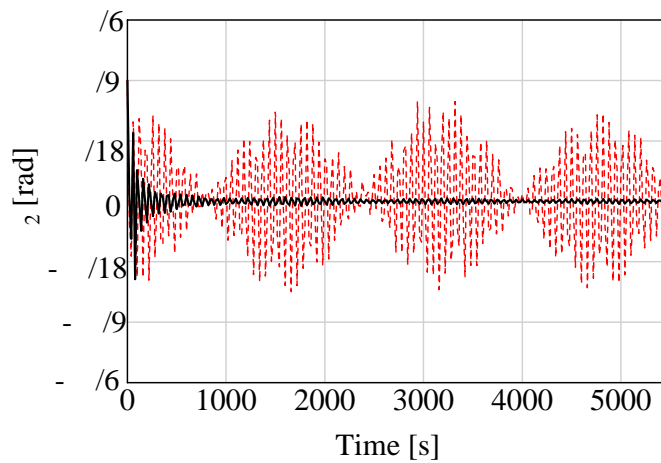
Fig. 10 Constellation Transition



(a) φ_2



(b) θ_2



(c) ψ_2

Fig. 11 Attitude Control

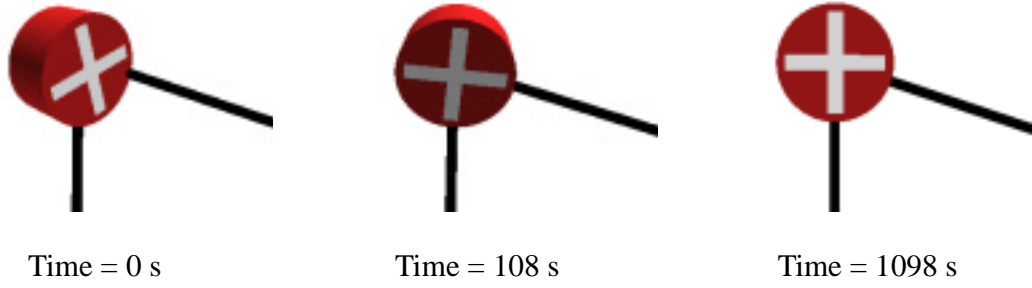


Fig. 12 Attitude Transition of Satellite 2

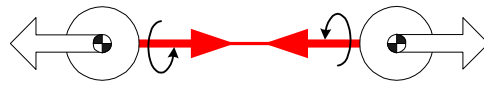


Fig. 13 Tether Twist ($n = 2$)

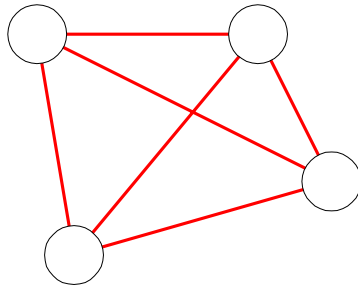


Fig. 14 Interaction between Tethers ($n = 4$)

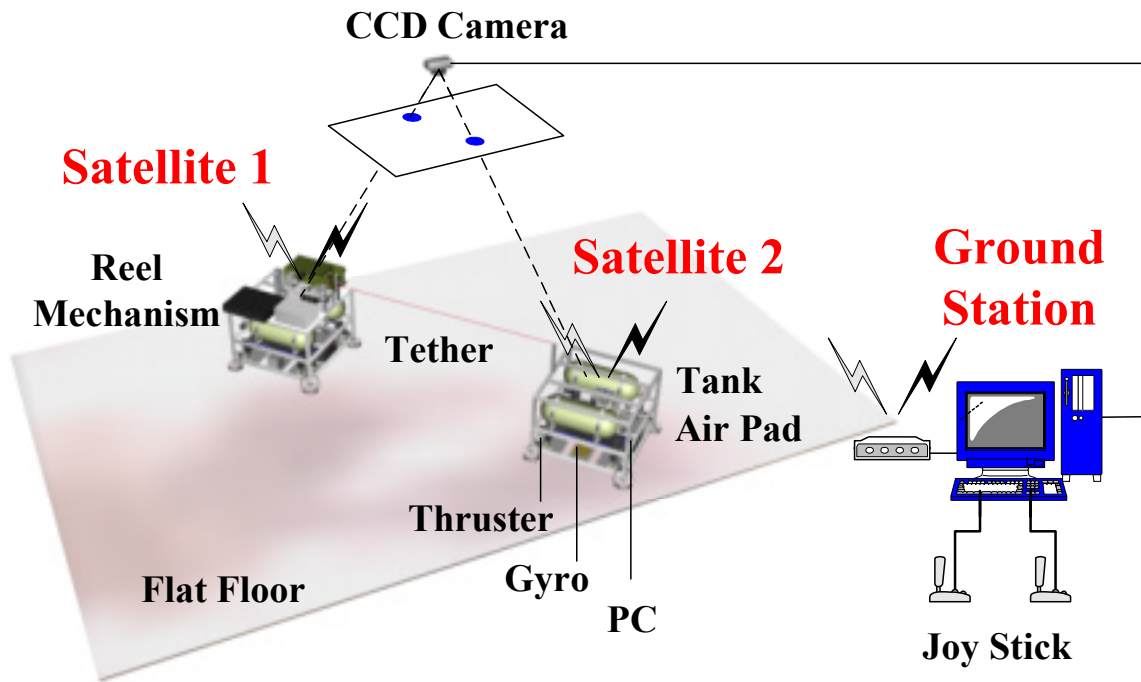
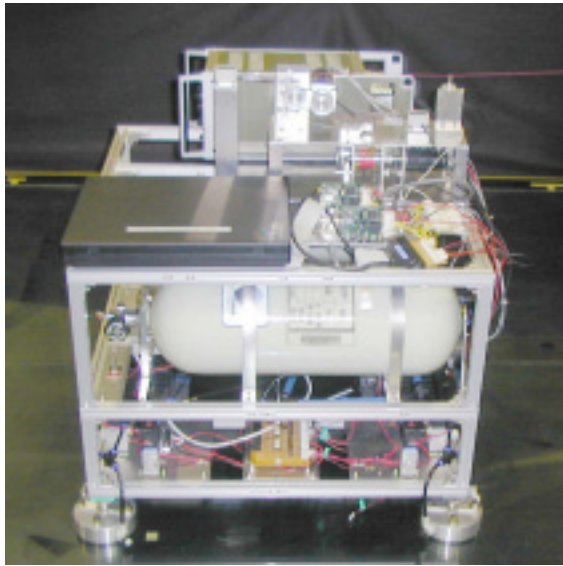
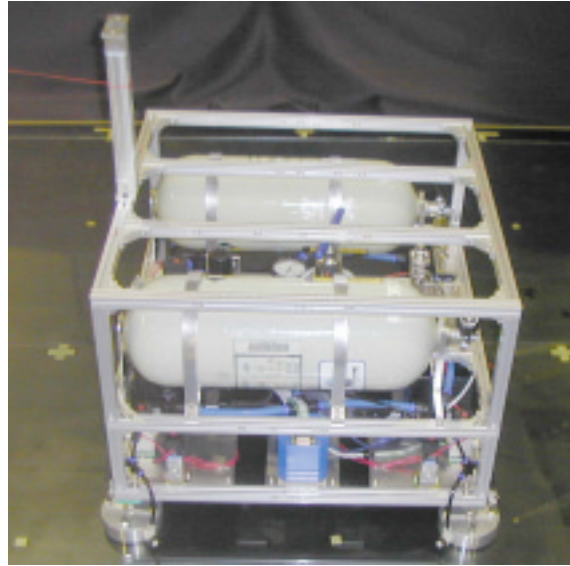


Fig. 15 Ground Experiment System



(a) Satellite 1



(b) Satellite 2



(c) Ground Station

Fig. 16 Subsystems

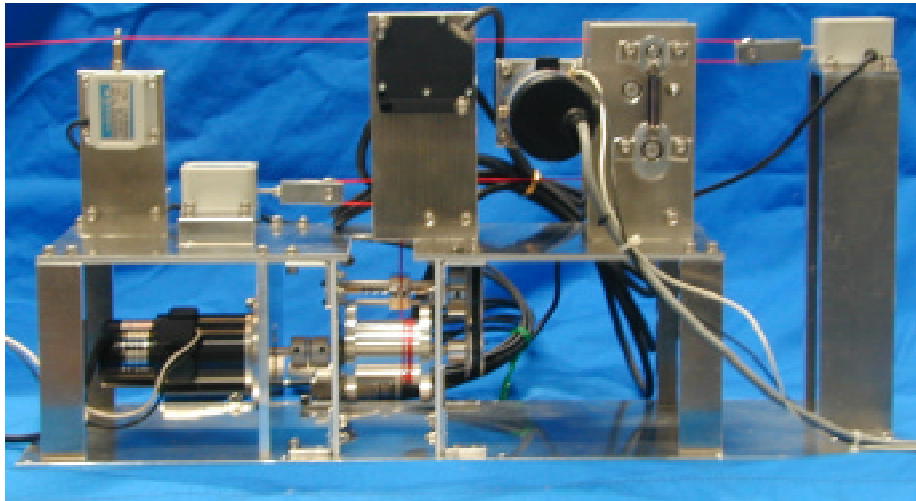
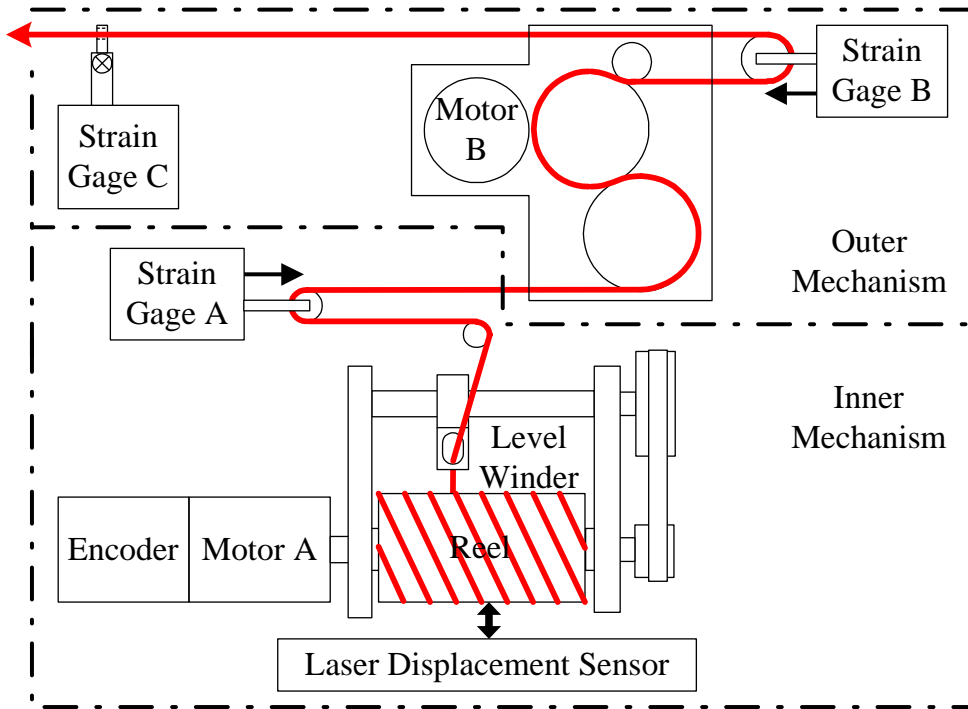
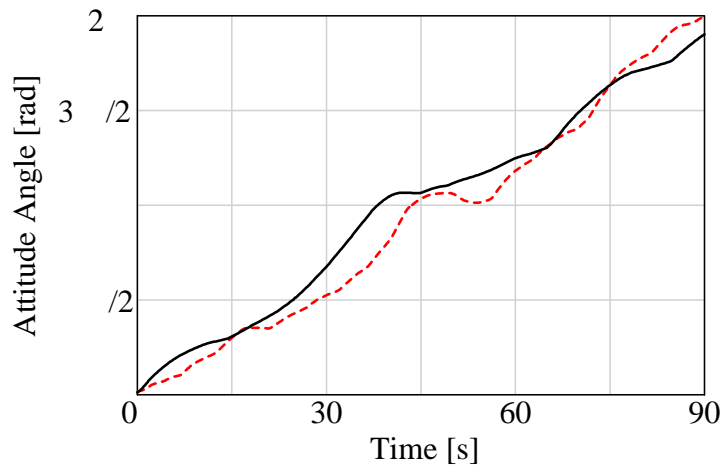
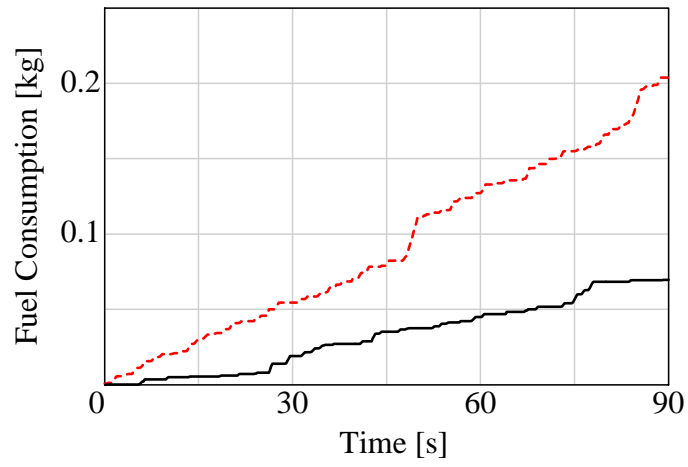


Fig. 17 Reel Mechanism



(a) Attitude Angle



(b) Fuel Consumption

Fig. 18 Experiment Results of Satellite 1

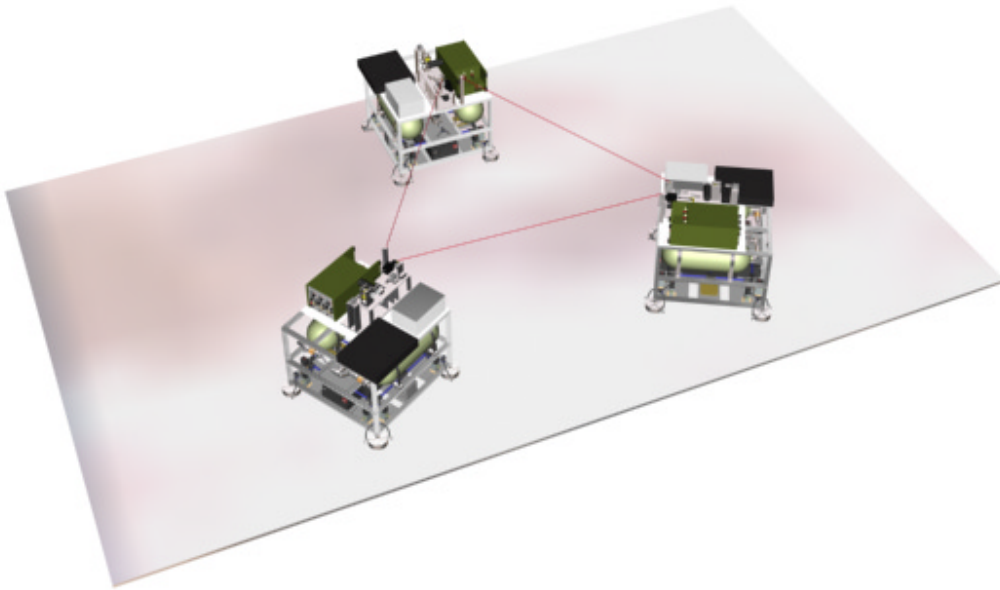


Fig. 19 Formation Flight Experiment

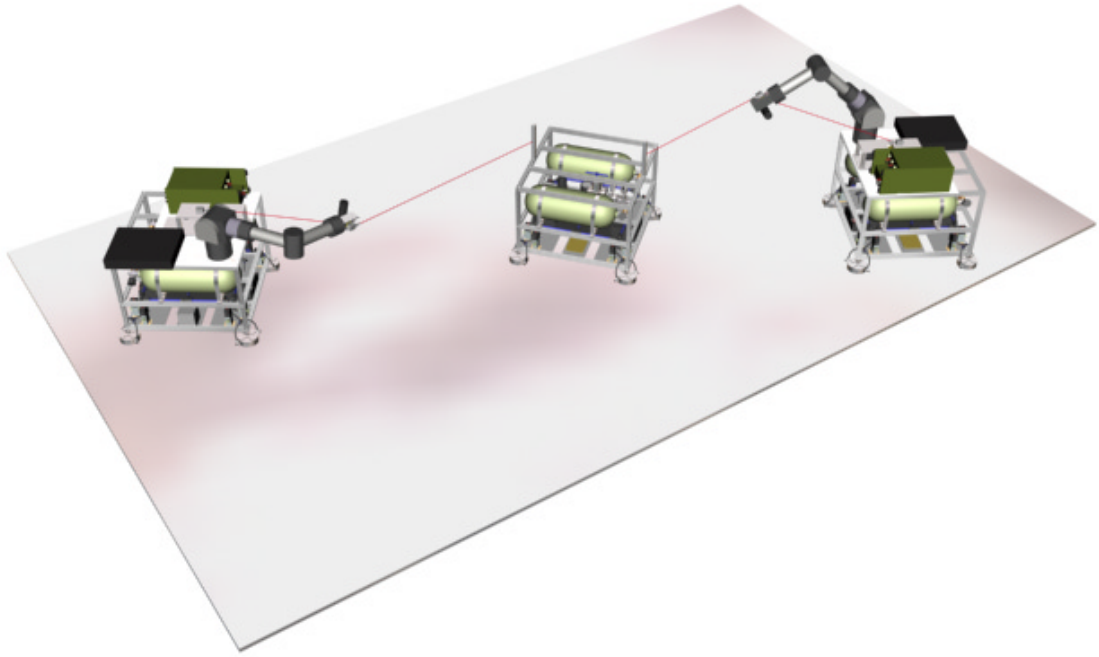


Fig. 20 Tether Service Experiment